Research Article Open Access

Jacques Gierak*

Focused Ion Beam nano-patterning from traditional applications to single ion implantation perspectives

Abstract: In this article we review some fundamentals of the Focused Ion Beam (FIB) technique based on scanning finely focused beams of gallium ions over a sample to perform direct writing. We analyse the main limitations of this technique in terms of damage generation or local contamination and through selected examples we discuss the potential of this technique in the light of the most sensitive analysis techniques. In particular we analyse the limits of Ga-FIB irradiation for the patterning of III-V heterostructures, thin magnetic layers, artificial defects fabricated onto graphite or graphene and atomically thin suspended membranes. We show that many of these early-pointed "limitations" with appropriate attention and analysis can be valuable for FIB instrument development, avoided, or even turned into decisive advantages. Such new methods transferable to the fabrication of devices or surface functionalities are urgently required in the emerging nanosciences applications and markets.

Keywords: FIB; Ga ions-solid interactions; nanofabrication

Doi: 10.2478/nanofab-2014-0004
received February 13, 2014; accepted May 08, 2014

1 Introduction

Finely Focused Ion Beam (FIB) technology emerged almost thirty years ago, amongst many other techniques, as a response to microelectronics "direct write" needs, for example in terms of photolithography mask repair [1]. At present, one must note that FIB techniques have become very popular, especially in the field of integrated circuit inspection and for failure analysis in electronic device manufacturing [2]. For this market, several companies have developed and made available FIB commercial tools starting in the middle of the 80's. In all these FIB machines, the emitted ions after extraction from a punctual ion source (mainly gallium) are successively transported, focused and scanned onto a sample with landing energies typically in the 30 to 50 keV range. When such gallium ions impact a material they will displace atoms from their normal positions in the solid, or in the case of a crystalline materials, from their lattice sites, and a "displacement cascade" is formed. As a result, various ion-target interactions like plastic deformation, swelling, mixing, milling, implantation, backscattering and nucleation will take place in the target substrate [3]. These effects result from energy and momentum exchanges between the incident ions and target atoms. Energy deposition and material modification are mediated by quasi-elastic scattering of ions with electrons, nuclei or whole atoms and their accumulation is primarily determined, in the case of FIB machines, by the incident gallium ions per point: the local ion dose/pixel. Accessing this local point dose, focused ions beams can be used in several versatile modes that are described in Figure 1.

1.1 Scanning Ion Microscopy mode

Initially and above all, a fine beam of energetic ions impacting a sample allows the observation or the examination of its surface material structure. It is well known that very rich information on local physico-chemical properties of imaged surfaces can be extracted from the very low ion/matter interaction volume [4]. This mode is generally referred as the Scanning Ion Microscopy (SIM) via collection of the secondary electrons re-emitted by the surface of the sample under ion bombardment. In this mode, a low number of ions per pixel (a few tens/pixel) are required to achieve high contrast and imaging spatial resolution (Figure 1a).

*Corresponding author: Jacques Gierak: LPN – CNRS, Route de Nozay, Marcoussis, France, e-mail:jacques.gierak@lpn.cnrs.fr

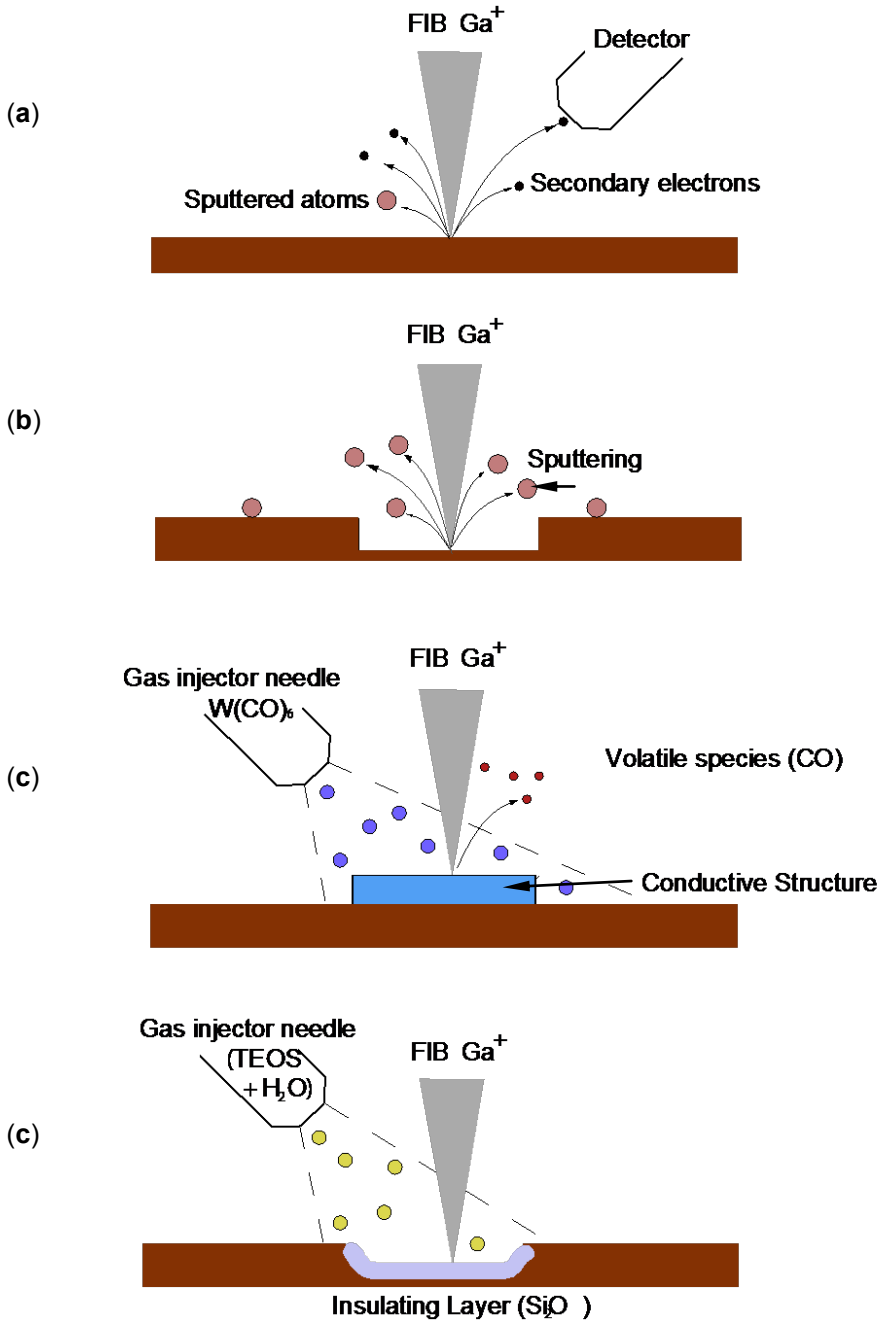

Figure 1: Schematics of the different FIB operation modes (a) Scanning Ion Microscopy mode. (b) Direct write or patterning mode. Deposition of respectively (c) conductive structure induced by decomposition of W(CO)6 gas or (d) insulating layer grown using combined tetraethyl orthosilicate (TEOS) and water vapour decomposition.

1.2 Direct write mode

The same ion beam can also be used like a lancet for resist-free, three-dimensional (3D) milling of patterns and operations. The general principle relies on exploiting the kinetic transfer of energy of an incoming ion and its momentum to target atoms through elastic and inelastic interactions. In the case of elastic interactions (nuclear energy loss), the energy of the ion is mainly transferred to the atoms of the target in the form of displacements. When the number of ions is increased to a few millions per impact the accumulated deposited energy causes collisional damage and subsequently sputtering phenomena at the surface of the irradiated targets (Figure 1b).

1.3 Local deposition of material mode

Finally, a FIB probe can also be used as a local supplier of materials (conductor or insulator) for Ion Beam Induced Deposition (IBID). This technique relies on an energy transfer mechanism occurring between secondary electrons generated by the ion probe impact on the sample surface and gas precursor molecules adsorbed on this surface. This energy transfer locally induces a "cracking" of the gas precursor molecules (Figure 1c & 1d). The non-volatile compounds resulting from this reaction, which are generally selected for their metallic or insulating character, form a solid-state deposit adhering to the surface of the target.

The addition of all these functionalities inside a single experimental setup makes FIB machines increasingly popular and invaluable in fields as varied as microanalysis, microscopy and direct prototyping or the repair of micro or nano-devices. As an example, using a FIB machine, it becomes possible to troubleshoot Integrated Circuits (ICs), replace failed connections and eliminate short circuits, all at a scale of only a few nanometres. These operations can be compared, at a much different scale, to what electronics engineers do when prototyping IC printed boards using wielding pliers and soldering irons [5]. Nowadays, FIB allows careful and precise analysis of failed points on densely integrated electronic chips, mainly to clarify the cause of failure for feedback to the design and manufacturing processes. In most cases, due to ever increasing IC integration, the defects causing the failure are located deep under the chip surface and most often between the surface and lower device layers. In such a case, precise surgery through dielectric films and metal wiring must be achieved with a full 3D control at a few tens nanometre scale. This procedure now fully automated is routinely performed using dedicated machines the FIB manufacturers have brought to the market.

2 Ion sources and FIB limitations, main development routes and alternative ions species

2.1 Ion sources and FIB limitations

What is important to note is that, even if the interest in the FIB technique has been continuously growing since the 80's [6], a list of limitations, warnings and drawbacks were almost immediately raised against this technique. In particular one could list limitations in terms of achievable throughput, patterning resolution, excessive or uncontrollable damage generation and in terms of pollution either caused by the incident ions (gallium in most cases) or by sputtered material re-deposition.

Practically, when a focused beam of gallium ions having an energy typically around 30 keV is scanned over sample surface to create a pattern through topographical modifications, high ion doses are required. A first consequence is that, mainly because of these high ion doses required (~ 10^{18} ions/cm^2) and of the limited beam particle intensity available in the probe, FIB etching based processes remain relatively slow [7, 8]. For most materials, the material removal rate for a 30 keV gallium ion is around 1 – 10 atoms per incident ion, corresponding to a machining rate of around 0.1-1 μm^3 per nC of incident ions. Therefore patterning throughput or material removal rates are limited in the μm^3/minute range.

The second disappointing consequence is that for most applications the spatial extension of the phenomena induced by Focused Ion Beam irradiation constitutes a major drawback. This damage generation was immediately pointed out, quite a long time ago [9], as the ultimate limitation for the realisation of highly localised structures by FIB. This was especially true and limiting with materials very sensitive to ion-induced defects, like III-V compounds. Numerous experimental results were found to converge towards the demonstration that ion damage penetrates much deeper than was expected from classical collision calculations [10]. Similarly, a lack of lateral selectivity for FIB direct patterning processes has been also evidenced and recently re-verified [11, 12]. This last effect was attributed to the existence of deleterious tails in FIB probes, extending up to the micrometre range. As a result a strong scepticism toward FIB technology was raised. Following this, the idea of using ions for nano-fabrication was considered as a pure dream only a few years ago and FIB direct patterning techniques deemed unable to enter the ambitious "nano" application field.

2.2 Main FIB development routes and alternative ions species

In opposition to the criticisms raised, one must note that FIB technology continuously expanded and has become the tool of choice in many fields starting with every IC foundry around the world and many laboratories concerned with TEM sample preparation, photonics, nano-fluidics, integrated circuit modification and MEMS. This success can be explained simply because process engineers, facing a lack of adequate tools and techniques, learned how to use FIB technology and how to unveil its formidable potential.

On the FIB machine development side, one must note that after flourishing early years in terms of academic research on ion physics and ion emission science, the main development effort was continued out by only a few companies, mainly concentrating their efforts on IC industry needs: their main market.

Final FIB user needs or market requirements were integrated over the years by manufacturers into design specifications for their commercial FIB tools. These can be summarized as follows:

(i) On one hand FIB/SEM machines must allow precise navigation on complex micro-circuit chips and unambiguous identification of the area of interest [13]. For achieving this precise FIB alignment both a sharp ion beam profile and a very low probe current are required for respectively optimizing image sharpness that is dependent on the Rayleigh criteria (contrast variation between two adjacent features) and preserving the sample. Indeed a low probe current prevents observed devices from being rapidly sputtered by the incoming gallium ions. At this stage it has been shown that a FIB probe can be optimized to allow imaging conditions with contrast variations of about 10% while transporting currents are as low as a fraction of a pico-Ampere. As a result, resolving power deduced from an image can be as small as 5nm, but this measurement does not at all stand for the capacity of the instrument considered to sculpt matter at that same scale [14]. This can be simply explained because the transported current in the ion probe is too low (less than 1pA) to overcome shot-noise effects [15].

(ii) On the other hand because of throughput specifications, IC routine inspection requires the FIB etching operations to be carried out in a minimum time. In this phase the highest possible probe current, compatible with a given spot size and pattern resolution, is needed for rapid and precise specimen milling. Applications such as thin lamellae preparation [16] for Transmission Electron Microscopy analysis and deep trench milling for scanning electron microscopy inspection, require the probe current to be set to the highest possible value. Using a gallium LMIS-based FIB with limited brightness, the charged particle optics have to be calculated, engineered and operated in a mode accommodating ion probe currents between several tens of nano-Amperes for reducing etching times, down to fractions of pico-Amperes for performing sample imaging. Such a large (10^4) current variation is made possible by using the so-called, "cross-over" optics configuration [17,18] that is the only one capable of delivering such a wide probe current range.

In the ion source area the Ga-LMIS were optimized accordingly to sustain emission current range, stability and lifetime meeting the requirements of these commercial FIB machines. Unfortunately their limited performance in terms of energy width (5eV), relatively large virtual source size (30 to 50 nm) and brightness (10^6 ions/cm².srd) are now pointed out as the weak link of the instrumental chain, thus encouraging several alternative ideas to be explored.

Regarding the development of alternative ion sources applicable to FIB machines, new options have emerged recently that can be briefly summarized as follows:

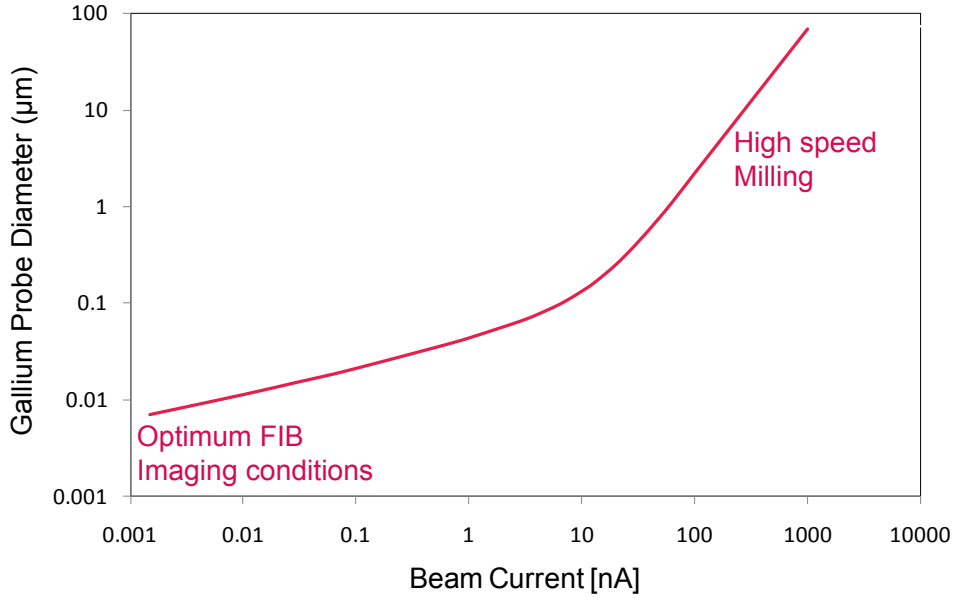

Figure 2: Illustration of the dependence of the probe diameter vs. the beam current for a commercial Ga-FIB machine and of the typical imaging / patterning operation mode. [Adapted from 44]

- *High current FIB machines*. FIB machines have been recently proposed using plasma ion sources for producing low temperature ions from a variety of gas species [19] having a normalized brightness exceeding 10^4 A.m²/srd.V for Xenon, $6.7.10^3$ A.m²/srd.V for helium, $4.5.10^3$ A.m²/srd.V for oxygen and $2.7.10^3$ Am²/srd.V for hydrogen. With probe currents in the micro-Ampere range, such plasma ion source technology allows considerably increased throughput over conventional gallium FIB instruments. Material removal speeds more than 20x faster when using the higher ion masses, site-specific cross-sectioning and large area milling, as well as sample preparation can be efficiently achieved. Therefore, these new high current FIB machines are receiving increased attention in the field of IC editing applications due to the high material etching rates they allow [20].
- *Helium Ion Microscope*. The possibility of employing a field emission ion source to produce a focused ion beam was first demonstrated in the early 1970's [21]. Several groups used a Gas Field Ionisation Source of the sort invented by [22] since it was realised that this arrangement would be ideal for developing a high-brightness, noble gas ion source with a low energy spread. GFIS rely on the field ionisation of the molecules attracted to a tip apex. Their virtual source size (1 nm) and the energy spread (< 1 eV) are significantly smaller than those of LMISs. Thanks to these performances, the FIB arsenal has been recently completed with the Helium Ion Microscope (HIM) capable of producing sub-nanometre probe sizes of low mass ions (He) having low energy spread and reduced optical aberrations. This ion microscope allows access to nanometre-scaled resolution. Unfortunately since helium ions are light, the sputtering rate is much lower than for a gallium beam. On the basis of TRIM simulations it has been shown that 30 kV gallium ions have a sputtering yield approximately 120x higher than He and 4x higher than neon at the same ion energy. To compensate and achieve more effective etching performance, Neon GFIS is now developed.

On the aspects of LMIS fundamental science & emission physics one must recognize that if there is a quite solid consensual understanding about the nature of the different intricate phenomena, their exact respective contributions in the global LMIS ion emission process remain quite unclear. For example one had to wait until recently to see decisive advances on the theory of minimum emission current for a non-turbulent liquid-metal ion source [23]. This recent important findings have allowed decisive breakthroughs in improving gallium-based LMIS geometry for low current emission [24]. On the basis of this improved LMIS emitter emission characteristics, we will review and detail the main limitations of FIB technology the author and his team are facing and how it shall be possible to take benefit of these and the single ion implantation perspectives.

3 The needs for a high performance FIB instrument architecture – Our route to a "Nano-Writer" concept

Before detailing the author's vision on high resolution FIB machines we will start by presenting the existing FIB tools available on the market. As already discussed above, because of main market requirements, the great majority of commercial FIB instruments are based on the highly successful combination of a Scanning Electron microscope with a FIB. This FIB/SEM architecture often referred to as "cross-beam" or "dual-beam" systems. In such setups the FIB column is attached to a SEM platform with the two column optical axis crossing at a same point on the sample. This combination provides milling (FIB) and observation capabilities (SEM). This architecture was invented in the middle of the 80's [25] and demonstrated efficient in-situ observation, non-destructive control and real-time monitoring of FIB processes [26].

However, with the advent of nanofabrication, new requirements in terms of positioning accuracy for the FIB spot, specimen motion and beam scanning strategies are necessary. For example FIB manufacture of structures wider that the elementary patterning field (squares a few tens of micrometres in length) may require the initial pattern into to be split into sub-patterns that fit in individual elementary writing fields. To achieve this, field stitching via re-positioning of each elementary sub-pattern with the writing resolution (some tens of nm) is often proposed. Concomitantly, FIB patterning of a large number of features in an automated way onto a pre-existent structure also requires high-precision positioning. Such tasks are difficult to control without adequate metrological positioning tools. Indeed the requirements here in terms of metrology are considerably more severe. In particular, in combined FIB/SEM systems the sample position at high tilt angles and the complex geometrical arrangements between sample and FIB column, which in some cases result in non-symmetrical electromagnetic fields, may impose some limitations.

Accordingly and especially for metrology and automation aspects, a "single beam" FIB architecture, equivalent to the well-known and highly successful systems used for electron beam nanolithography, the so-called "nano-writers" have to be preferred [27, 28].

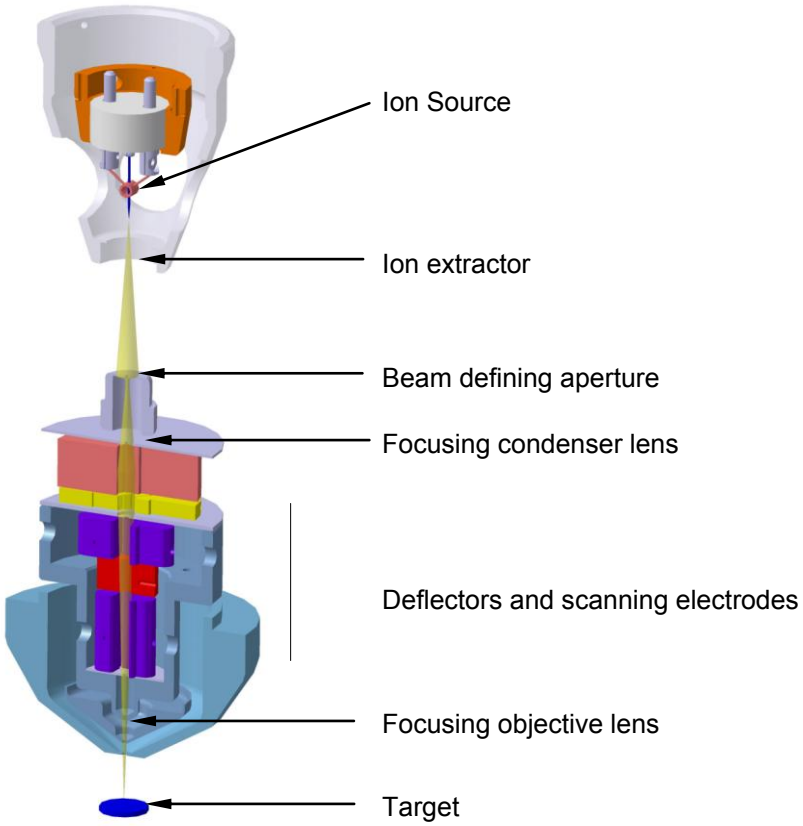

Figure 3: Schematic view of the high resolution two-lens Focused Ion Beam column using a Liquid Metal Ion Source designed for matching original "nano-writer" specifications from LPN-CNRS [29].

Following the analysis reported above, and in the light of the experience gained in our team since the middle of the 80's, in terms of LMIS research, FIB instrument development and emerging FIB applications, some years ago we came to the conclusion that for our research purposes a dedicated FIB concept optimised solely to deliver highest possible patterning resolution was necessary. The "nano-writer" architecture was selected and a complete system was engineered to allow state-of-the-art performance level in nano-patterning using gallium ions.

The specific FIB column and ion optics concept is schematically presented on Figure 3. Ion optics usually involves electrostatic lenses and deflectors, which consist of several circular electrodes with high voltage applied to the central one. This high voltage is usually about half of the beam potential and requires specific design precautions. The most interesting property of these lenses is that they have a focusing action that is independent of charge-to-mass ratio. Because of the large energy width of the emitted beam, chromatic aberration appears to be the main limitation when attempting to improve the beam resolution. The FIB optics was designed using a high-performance optical architecture we have proposed some years ago for high-resolution FIB systems [30]. In this FIB optics design, the ion source and the electrostatic optics are independent and allow the ion energy to be set in the range 30 to 40 keV. Focusing is achieved through two asymmetric lenses operated in the decelerating mode and in infinite magnification conditions (non-cross-over mode). Since the "nano-writer" architecture allows for a compact column design, we have designed a short (~50 mm) optics with deflection plates located between the lenses, allowing a reduction of the final lens working distance (WD), a necessary condition to achieve a strong demagnification of the non-negligible Ga-LMIS virtual source size. The performance of this high-resolution ion optics column was initially calculated for various configurations using state-of-the-art theory and modelling software [31]. For our optimized gallium LMIS the results are as follows: for a beam voltage V = 40 kV, an ion source size δ = 30 nm, an energy spread of the beam ΔV = 5 eV, an acceptance angle aO = 0.1 mrad and a focusing angle aP: 0.84 mrad, the source magnification: $d_G = M \cdot \delta$ ~3.5 nm.

The disks of least confusion for chromatic and spherical aberration can be respectively expressed as:

$$d_{chromatic} = C_C \cdot \frac{\Delta V}{V} \cdot \alpha_o = 2.93 \text{ nm} \quad \text{and} \quad d_{spherical} = \frac{1}{2} C_S \cdot \alpha_o^3 = 0.03 \text{ nm}$$

For the addition of the various contributions, it has been usual in the past to estimate the resulting spot-size by adding the individual contributions in quadrature:

$$d = \sqrt{d_G^2 + d_C^2 + d_S^2}$$

But this is known to be a crude estimate. A better estimate is obtained from the expression:

$$d_p = \left[\left\{ \left(d_D^4 + d_s^4 \right)^{\frac{1.3}{4}} + d_G^{1.3} \right\}^{\frac{2}{1.3}} + d_c^2 \right]^{1/2}$$

In the absence of any diffraction contribution and a negligible spherical aberration term, this collapses to the quadrature value of about 5 nm.

4 Physics in nanometre-scale FIB patterning

For nanometre-scale FIB patterning, the appropriate level of interaction between ions and solids is translated towards low dose effects. Collisional defects in the vicinity of the surface irradiated layers play the major role here. This is due to the shrinkage of the lateral dimensions, to the very small thickness of the active layers used and to the extreme sensitivity of these materials towards ion bombardment. Indeed most of the target materials involved in nano-fabrication experiments are very sensitive to ion bombardment. This is the case for III-V crystals, thin magnetic crystalline films or inorganic compounds with weak bonds, ultra-thin membranes or even atomically suspended sheets of graphene and h-BN. All these sophisticated materials exhibit very high ion sensitivity well below the 10^{18} ions /cm² range traditionally required in gallium FIB milling applications (30 to 50 keV Ga^+ ions). The creation of defect cascades and other irradiation-induced defects has often been considered as a limiting factor in the application of FIB technology. This is especially true for ion-milling. Under these conditions, the FIB patterning capability cannot be directly extracted from the measurement of the incoming ion probe diameter, as the lateral expansion of the defects induced by the impact of the ion beam can considerably exceed the initial probe size.

In the following part we will review, detail and summarize the main path explored by the author and his collaborators, to assess and deduce from experiments the practical FIB nanofabrication limits against emblematic challenges in nanosciences.

As a second step, the structuring potential of our highly focused gallium ion beam was assessed and limits evidenced. Building on an interactive feedback with several collaborative groups we have been over several years collecting information and extracting data assessing the validity of a plurality of FIB configurations from the ion source configuration, to the optics settings and design down to the patterning strategies. This path lead to the optimization of the FIB "nano-writer" presented above, but also has allowed the design of a FIB system capable of achieving the highest possible patterning resolution [29].

The related vision was that controlled and reproducible fabrication of nano-structured materials would constitute one of the most crucial industrial challenges for the broad dissemination of nanosciences advances in the fields of nano-electronics, nano-optics and nano-biology/nano-medicine.

4.1 Probing the spatial resolution of Focused ion beam irradiation using III-V Multi Quantum Wells or two-dimensional electron gases.

It is widely accepted that the spatial extension of the phenomena induced by FIB irradiation is limiting the use of this method for the realization of highly localized structures. Indeed, when FIB technology was introduced in the end of the 70's, a promising future was immediately foreseen, specifically for in-situ structure realization and epitaxial growth of high quality semiconductor [6]. Several attempts aiming at combining in a single tool local doping and local etching with 3D control (FIB) together with molecular beam epitaxy of high quality III-V semiconductors were carried out [32]. But several basic limitations of the FIB technology were rapidly pointed out related to a lack of selectivity, and limited patterning throughput. Indeed, damage penetration was found to be one order of magnitude deeper than what classical calculation in amorphous media would predict [10,33]. These observations were partly explained on the basis of channelling effects, but in the transverse direction, an even worse lack of lateral selectivity for FIB direct patterning processes on III-V compounds was later evidenced [11].

Indeed FIB-induced damages spreading up to 4 μm away from the impact were detected and explained by the existence of deleterious tails in FIB probes. These tails

induce a lateral spreading of the ion beam damage in a few micrometre range. After careful investigations of the focused ion beam induced damage distribution through theoretical calculations and cross-sectional transmission electron microscopy in III-V crystals our beam profile that was deduced for a 30 keV Ga^+ ion probe was found to follow approximately a Gaussian shape at low emission currents (< 5μA) [34].

In order to get a better understanding of the lack of selectivity of the FIB patterning process, we have then investigated the influence of the sample temperature during FIB irradiation by using multi quantum wells structure (MQWs) as sensors. In a GaAs/GaAlAs MQW structure, three quantum wells having different thicknesses and located at different depths were used as high sensibility sensors, in relation to the damage created during the FIB irradiation through low temperature photoluminescence (LT-PL) intensity measurements. FIB irradiations were repeated for the exact same FIB conditions on a same sample at a very short time interval (~30 minutes) successively kept at room temperature (300K) or at 80K. FIB-induced longitudinal and lateral damages were then probed directly after irradiation without subsequent annealing procedure of the sample. The FIB-induced damage profile evolution between an irradiation performed at room temperature (300K) and at 80 K is presented on Figure 4.

The details of these experiments that are presented elsewhere [35] can be summarized as follows: Both longitudinal and transverse characterisations show that defect diffusion exists during FIB irradiation at room temperature. The longitudinal diffusion length of the defects at room temperature is around 100 nm, while it reaches a value of 900 nm in the lateral direction. The relative measured defect extension is much higher in the lateral direction than in towards depth. This anisotropy can be attributed to an enhanced diffusion of defects in the aluminium rich MWQ interface. We came to the unexpected finding that both lateral and longitudinal defect profile extensions are drastically reduced when FIB irradiation is operated on a sample kept at low temperature. This clearly evidences the advantage of low temperature implantations, when damage injection must be highly localised.

Application of this method to the patterning of wires into a two dimensional Electron Gas (2DEG).

To assess the potential and the limits of FIB technique for low dimensional structures fabrication based on FIB-induced disordering of quantum wells, we have patterned a 2DEG kept at an even lower temperature (22 K). Arrays of parallel 100 μm long wires were defined (Ga ions, 30 keV, ion dose 10^{15} /cm²). Channels were written along the current axis of a deeply mesa-etched Hall bar pattern with selected widths ranging from 5 μm down to 0.1 μm. The resistance of the patterned wires was then measured at low temperature (4 K) again without any sample annealing process. Finite layer resistivity were measured even for channels having widths as small as 0.5 μm. (R=1.7 MΩ at T = 4 K), attesting that the 2DEG are preserved in such sub-μm FIB-defined channels.

From these tests attempting to structure III-V semiconductors MQWs and 2DEG, we can extract the following information:

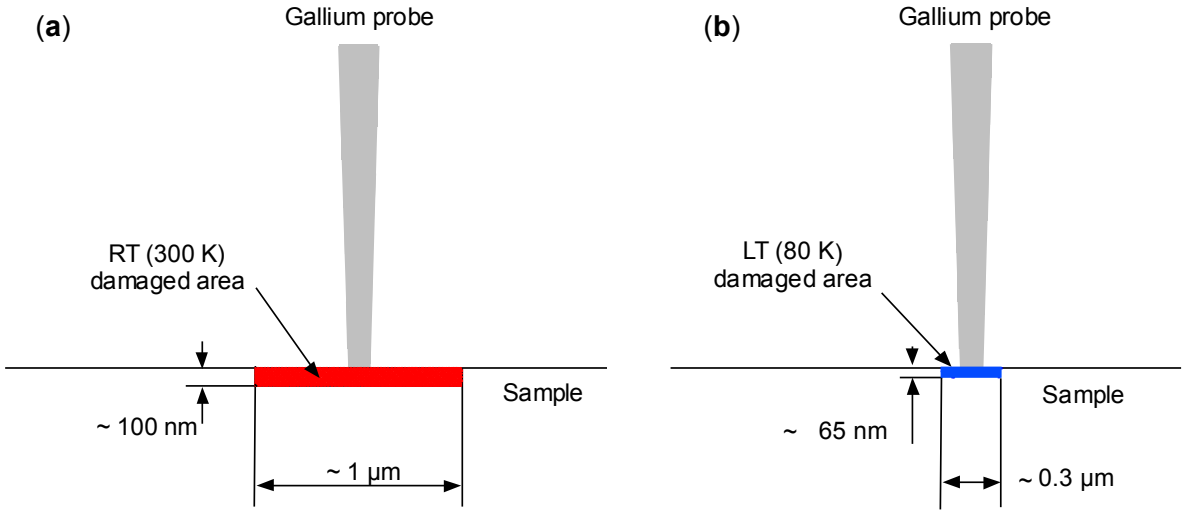

Figure 4: Schematic variation of the damage profile injected by a 10 keV gallium FIB on a GaAs/$Ga_{0.67}$ $Al_{0.33}$As MQW grown by MBE. (a) Damage profile for a sample kept at room temperature (300K) and (b) at 80K during the FIB irradiation. Damages are probed using low temperature (4K) Photoluminescence.

- Highly sensitive devices such as 2D electron gases can be processed at dimensions compatible with nanofabrication if the sample is kept at cryogenic temperatures (< 100 K) during FIB patterning.
- FIB induced defect diffusion and damage spreading can be anticipated and managed.
- FIB patterning effects relying mostly on highly directive channelling effects are possible.
- The so-called "long tail theory" or "broad exponential tail" previously raised was not confirmed. It became realistic for us to develop nanometre sized FIB probes.

4.2 Magneto-Optical Microscopy (MOM) as a tool for probing FIB irradiation damage

In coll. with A. Mougin et al. Laboratoire de Physique des Solides, UMR CNRS 8502, Université Paris-Sud, F-91405 Orsay, France

Thin magnetic Pt/Co/Pt structures have been reported to be very sensitive to ion irradiation, allowing controlled changes to their magnetic properties [36]. These changes were ascribed to progressive modification of the Co atom environment near the Pt/Co interfaces, due to the elastic collisions induced by the ion irradiation often referred as ''ion beam mixing'' [37].

Pursuing our efforts in understanding the limits of high resolution and low dose FIB patterning we then started to explore the potential of our FIB machine against magnetic nano-structures fabrication. This applicative domain is a challenging area for recording and memory applications, but also for basic research on nano-structures.

Concomitantly on the FIB technology side the physics of the magnetic properties changes in ultrathin magnetic layer structures driven by ion irradiation allowed us to compare our FIB operating parameters and configuration with an unparalleled sensitivity.

As an example, bombarding a Pt(3.4nm)/Co(1.4nm)/Pt(4.5nm) sample for each incident 30 keV Ga^+ ion about 650 Pt or Co atoms are removed from their original lattice sites in the Pt/Co system. Ion irradiation causes a progressive reduction of the perpendicular magnetic anisotropy, coercivity and Curie temperature.

These effects can be probed thanks to the extreme Polar Magneto-Optical Kerr (PMOKE) sensitivity to the nonlinear variation of the signal when working in the vicinity of the Curie temperature. PMOKE microscopy on a Co/Pt target yields a detailed mapping of the spatial incident ion distribution for extremely weak Ga ion irradiation. The statistical character of the irradiation process, involving a small number of Ga ions per spot, can therefore be studied at very low dose. Statistical effects and local disruption of the magnetism in nanostructures are indeed of the highest importance when assessing the ultimate patterning potential of our technique.

To give a clear picture of this dramatic effect induced by FIB irradiation on a virgin Pt/Co(1.4nm)/Pt film that is a rather hard ferromagnetic material with a coercitivity (*Hc*) ~ 300 Oe. After this film is irradiated with gallium ions and a surface dose as low as $D = 8.10^{14}$ ions/cm², the film is transformed into a soft ferromagnetic material (*Hc* ~ 20 Oe).

Finally the film can be turned to paramagnetic for $D > 1.5.10^{15}$ Ga ions/cm² (Figure 5). At this point one must keep in perspective the extremely low ion doses, down to a few ten of ions per impact that are used. In comparison, traditional FIB milling processes require ion doses that exceed 10^{18} ions/cm². Then the perspective opens to obtain significant areal information-density enhancement without signal-to-noise ratio degradation related to an increase in surface roughness. The FIB patterning technique allows one to define arrays of nanometre-sized dots and lines with identical geometry without modifying the surface topography too much. These model systems were tested in order to investigate such fundamental questions as magnetic inter dot coupling, reversal dynamics and dipolar interactions of sub-micron magnetic elements

One important goal was to isolate magnetically stable domains organized in a matrix. To achieve this, the beam of Ga ions was scanned along arrays of horizontal and vertical lines defined with fixed intervals. Our initial idea was to use the sputtering effect of the gallium beam to etch a boundary line in between two adjacent domains. This idea was tested but immediately discarded. The low patterning speeds we measured (a few μm/s or less) were not compatible with the reproducible patterning of a sufficient number of magnetic elements (10^4 to 10^6). Moreover, re-deposition of sputtered contaminating materials and, in some cases, charging effects causing shifts was evidenced. Additionally, the initial flat surface morphology of the film was to be preserved, in order to ensure a maximum compatibility with potential magnetic reading/recording processes. A similar problem was evidenced when the magnetic film is pre-covered by a carbon layer for additional protection [38]. In addition to the added thickness reducing the ion-induced mixing efficiency, implantation of carbon from the overcoat into the Co layer becomes significant along with the relatively high Ga dose required for milling, as the etching of trenches becomes necessary.

In parallel, we decided to pursue the exploration of an original patterning route for magnetic layers, based on an ion beam mixing process. Lines were realized via

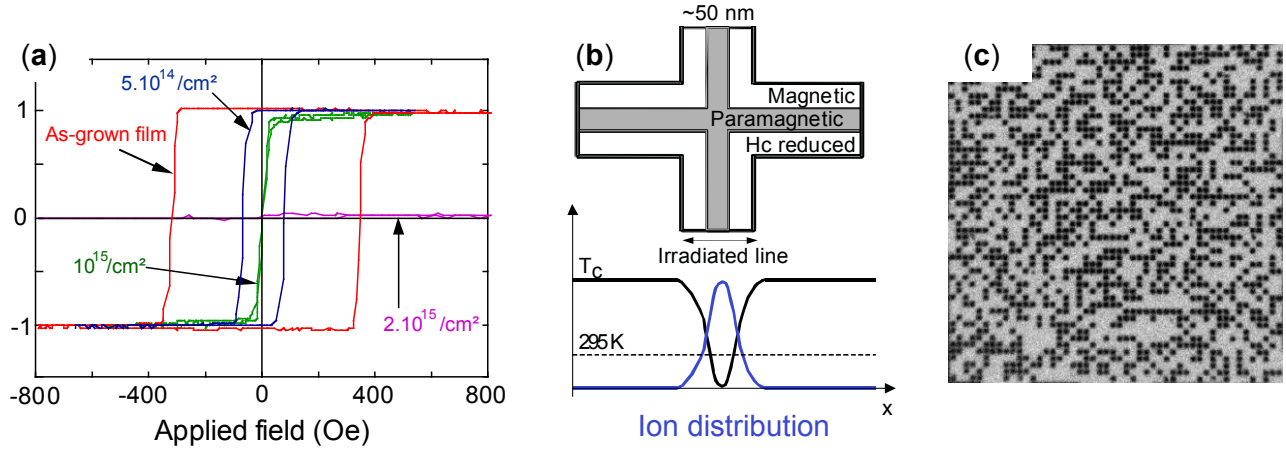

Figure 5: (a) Faraday hysteresis loops for a Pt/Co(1.4nm)/Pt film comparing as grown and different Ga-FIB (30 keV) irradiation doses. (b) Schematic view of FIB magnetic lines separating the magnetic dots. In the middle of each line ion fluence is large enough to render the Co layer paramagnetic (Grey). At line borders ion dose is lower the material becomes magnetically softer. (c) Magneto Optical image of magnetic domains patterned (50 x 50 μm²).

digitally scanning the Ga^+ probe with a pixel time and pixel-to-pixel distance set to values ranging from 1.25 10^{16} ions/cm²down to 1.25 10^{15} ions/cm². These low ion doses, allowing writing speeds of about 0.08 mm/s and 80 mm/s respectively, were used for samples containing a single Co single layer. For magnetic multilayer samples having an even higher sensitivity, record writing speeds up to 200 mm/s were reached. This is to our knowledge a record for all scanning probe techniques.

Using the Ga-FIB technique delivering a sub-10 nm spot size we were able to fabricate stable magnetic patterns and have shown that the magnetic properties of a thin Co/Pt layer can be modified and progressively controlled using Ga-FIB irradiation with sensitivity down to 10^{12}ions/cm². That is one million time lower than ion dose used in classical FIB etching. Realizing boxes allowed us to probe the lateral extension of the intermixing effects. Such a high sensitivity to ion bombardment combined with precise measurements was found to be very useful way to calibrate and compare the performances of different FIB machines and for the comparison of different ion optics configurations and settings of a same FIB machine [39].

From this second experiment the following information can be extracted:

- Ga-FIB induced collisional intermixing can be localized at a few tens of nanometre scale and controlled to allow progressive and strong alloying of thin sandwiches of Pt/Co/Pt layers.
- Ga-FIB induced collisional intermixing is very efficient for the conditions described above and allows record writing speeds to be achieved.
- Sensitive materials and processes could be used to extract a faithful image of the incoming FIB ion distribution containing and stable magnetic nanostructures are fabricated using ion doses as low as only a few tens of ions per impact.
- FIB patterning is in this case not limited by ion source shot noise effects [40].

4.3 Artificial defects engineering using FIB

In coll. with J.M. Benoit et al. Institut Lumière Matière, UMR5306 CNRS, Université Claude Bernard Lyon 1, Domaine Scientifique de La Doua, Bâtiment Kastler, 10 rue Ada Byron, 69622 Villeurbanne, France

The design and fabrication of quantum dots systems and the study of their properties are playing an increasingly important role, mainly because of the large number of potential applications in various fields. Several approaches to produce such systems have been developed, including top-down, bottom-up or combined top-down /bottom-up technologies. Some years ago we were proposed to test using the FIB some functionalized substrates: 2D arrays of traps (defects) organized in arrays. Moreover specific geometries for the ion-induced defects had to be defined in terms of abruptness and spatial resolutions both typically in the 1–10 nm range.

For these experiments a Highly Oriented Pyrolitic Graphite (HOPG) sample surface was modified by FIB irradiations with a sub-10 nm probe size and very low ion dose. Our aim was to evidence and characterize the effect of a few gallium ions impacting on a highly crystalline surface and therefore to evaluate the possibility to create localized surface modifications, i.e. FIB-induced artificial defects.

The basic pattern design used here consisted of a matrix of points (dots) defined using a fixed step size and a constant point dose inside a same pattern; Due to the highly flexible methodology allowed by direct write FIB technique and the rigorous metrology allowed by our nano-writer instrument, the patterns were repeated in very large numbers, with parameters following a pre-defined variation law. Additionally unambiguous identification of milled marks and metrology calibration structures were added to allow easier identification or localization. Indeed effective area of interest localization is extremely important when using high resolution Scanning Tunneling Microscopes or Atomic Force Microscopes.

Initially the nature of the minimum detectable gallium ion-induced modifications was unknown. For this reason we started with patterns of high ion point doses to promote ion sputtering and create nano-holes in a material as resilient as HOPG. The dose was then progressively reduced within a set of patterns to very low ion point doses in order to investigate the influence of crystal amorphisation effects. The beam writing strategy was organized to generate a point matrix pattern having a constant distance between impacts. The pixel dwell-time for a 5 pA probe current was varied from 10 ms to 1.6 µs, corresponding to 3.10^5 and 50 ions/pixel respectively.

Tapping Mode Atomic Force Microscopy (TMAFM) was then used to investigate the defect morphologies. As expected we have observed that the defects created on the surface of the crystalline graphite substrate were dependent of the ion dose injected at each site [41]. As a matter of fact, for the highest ion doses, holes were etched into the sample and substrate material re-deposition and swelling were observed around the FIB etched holes, leading to a volcano-crater-like morphology. Conversely, for lower ion doses, only ion-induced defects and subsequent only local volume variations corresponding to surface modification were evidenced (Figure 6). These defects were identified as bumps having diameters measured at Full Width at Half Maximum of a few tens of nanometre. These observations have demonstrated that reproducible and tailored artificial defects having sizes in the few nanometres range were reproducibly fabricated using surprisingly low gallium irradiation doses. Using such artificial defect templates engineered with FIB

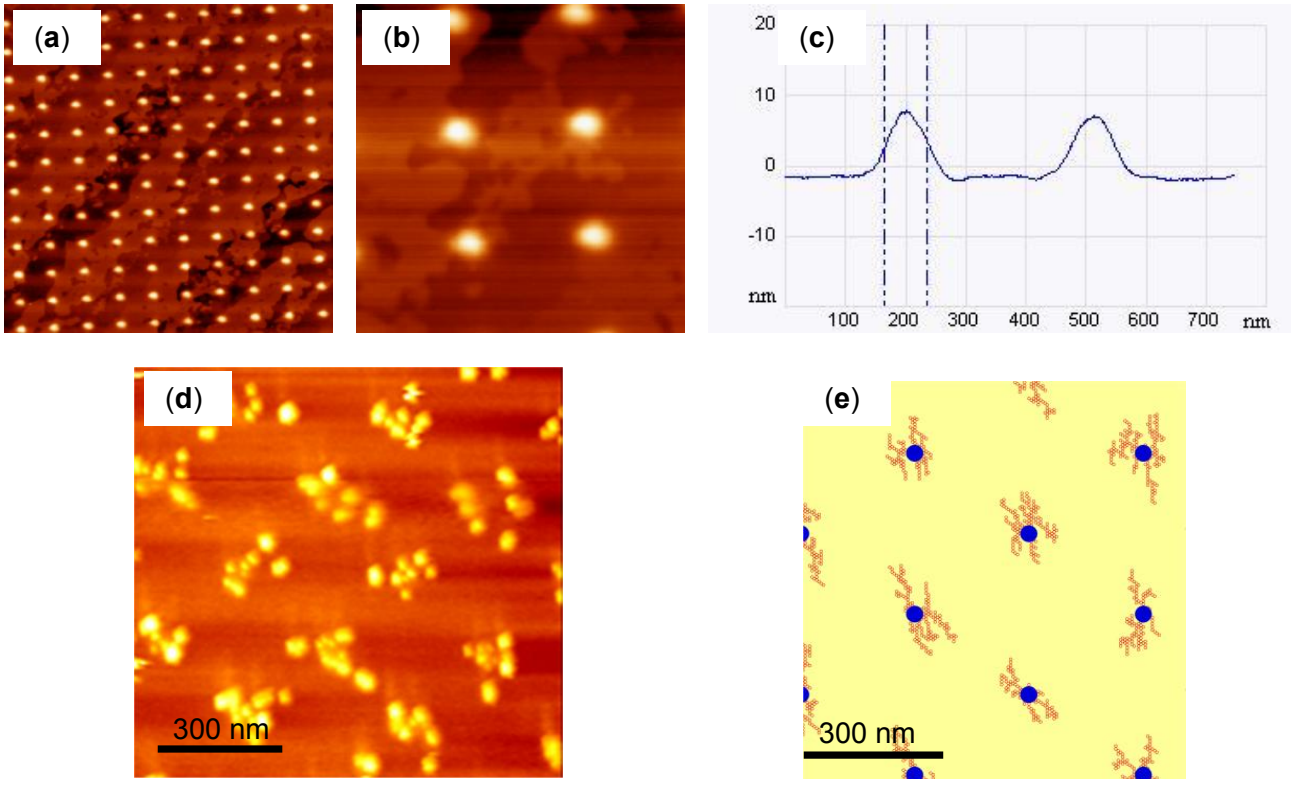

Figure 6: AFM topography image and profiles of a same array of defects created by FIB on a HOPG layer. (a) 3µm x 3µm AFM image of defects fabricated with a 300nm spacing. (b) Enlarged view (800nm x 800nm), ion dose of impacts realized for 2.10^5 ions/point. (c) Profile of the defects showing reproducible height of 8 to 9 nm and a 70 nm Full Width at Half Maximum. Comparison between experimental (d) and KMC-simulated (e) morphologies of gold (750Au) clusters deposited on FIB-induced artificial defects on a Highly Oriented Pyrolitic Graphite surface. Simulation is achieved with irreversible sticking (ideal traps).

controlled irradiation, local "guided" organization of diffusing metal clusters was observed and modelled (Figure 6e) [42].

From this step we learned that it is possible to:

- Organize, shape and control artificial defects using impacts generated by Ga ions.
- Retrieve these defect arrays fabricated if a rigorous metrology and organization is used for defect placement.
- Artificial defects acting as traps open new processes we have summarized as "guided self-organization".

As a complement to these experiments, one important limitation arising from the nature of HOPG substrates can be now solved by using graphene films grown on 6H–SiC(0001) substrates. Indeed using a finely focused gallium (Ga^+) ion beam, similarly to HOPG samples we have demonstrated the possibility to fabricate similar organized arrays of nano-defects designed using ion doses in the range of 10^6 Ga^+ ions/dot.

Using Conductive Atomic Force Microscopy (CAFM) and Raman spectroscopy we have evidenced the strong resilience of graphene towards ion irradiation and the electrical conductivity modification around FIB impacts.

Indeed such FIB defects written on graphitized substrates acting as nucleation centres, whatever the nature of the diffusing clusters, open the perspective to perform arrays of a large range of functionalized nanoparticles. [43]

4.4 Ultra-thin membranes and atomically-thin sheets as ideal templates for FIB nano-processing and probe visualization

In coll. with L. Auvray, F. Montel et al. Laboratoire Matière et Systèmes Complexes, CNRS - Université Paris Diderot, France.

FIB milling of a membrane is interesting if the membrane can be made homogeneous, conductive and thin enough; i.e. with a thickness comparable or ideally, well below to the projected range of the incoming gallium ions [45]. In this case the amplitude and the development of the collision cascades are significantly reduced while material removal and ejection mechanism allow comparison to the bulk target case.

To get a clear picture of the situation one must consider the fundamentals of ion implantation. In our present case of 30-35 keV gallium ions impacting and penetrating a sample, these ions are scattered at random angles and loose kinetic energy due to nuclear collisions as illustrated on Figure 8. A stopping power *S* can then be defined as the energy loss per unit length of the ion path as follows:

$$S = \left(\frac{dE}{dx}\right)_{nuclear} + \left(\frac{dE}{dx}\right)_{electronic} = S_n + S_e \approx S_n$$

This simplification *Sn + Se ~ Sn* is valid in our case of low energy (30-35keV) Ga^+ ions. This stopping power will define an average penetration depth from the surface where the gallium ions stop also called the projected range. This parameter can be then expressed as follows:

$$R_p = \int_{E_0}^{0} \left(\frac{dE}{dx}\right)^{-1} dE$$

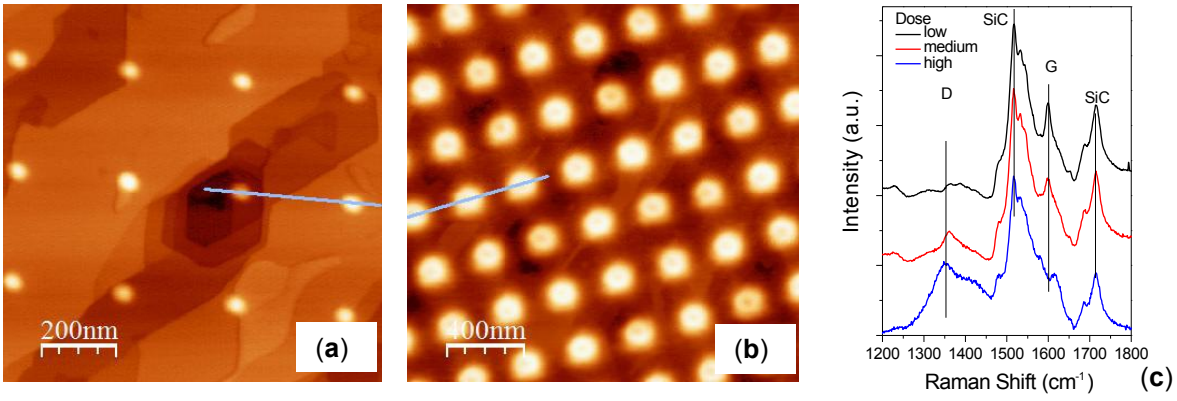

Figure 7: AFM topography images of defects created by FIB on a graphene film grown on 6H–SiC(0001) substrate for an ion dose about (a) 10^4 ions/dot and (b)10^6 ions/dot. (c) Raman spectra of the evolution of the D & G bands of an epitaxial graphene irradiated for increasing point doses. While increasing the dose, the relative intensity I_D/I_G increases indicating the presence of an increasing number of defects and G band downshift indicating stress modification in the epitaxial graphene layer (35 keV Ga+ probe current 6 pA).

In the case of gallium ions, the well-known SRIM code [3] gives precise estimations, but a crude estimate for a 30 keV gallium ion gives about 1 nanometre/keV. Considering this estimated value it can be predicted that membranes having thicknesses reduced below 30nm will progressively appear more and more transparent and will transmit some of the 30 keV gallium ions impacting. Additionally, in such a reduced target depth, the ion-induced collision cascades and scattering effects do not propagate very far and are therefore limited both longitudinally and laterally. This simple model predicts better ion-deposited energy localisation and a reduction of straggling effects for thin lamellar targets. In addition FIB processing of ultra-thin membranes allows some interesting technical features schematically represented on Figure 9a.

These advantages can be listed as follows:

- Material removal is facilitated since a collision cascade developing from the upper side of the membrane will not obviously propagate below the lower side, therefore forward sputtering is favoured. Engraved material is efficiently ejected; thus allowing very sharp edges to be obtained
- There is almost no possibility for sputtered material to re-depose on the backside of the foil since these particles are ejected with a highly directive transfer of kinetic energy.

Nevertheless, in attempting to fabricate nanometre-sized features we have observed two distinct situations:

4.4.a. Si-based thin suspended membranes including SiN, SiC and SiO2 can be easily drilled using FIB irradiation in order to fabricate arrays of pores or even one single nanopore. To achieve successful fabrication of nanopores in Si-based thin membranes a first requirement is to select membranes that are planar to keep a constant focus distance and low stress for resisting the mechanical stress modifications induced by the ion beam patterning. Fabricating the smallest possible nanopores in Si-based thin windows raises further requirements for the FIB to meet. The first one relates to the variation of membrane thickness within a single batch (2 to 5 inches wafers), making precise dose calibration difficult. In our case using our calibration technique described elsewhere [46], sub-10 nm nanopores can be fabricated reproducibly using a variable dose matrix and small increments in dwell-time.

A second important observation is that when using a narrowly focused beam of gallium ions (30-35 keV), the membrane grain size governs the minimum obtainable pore diameter. Nanometre sized-grains of the Si-based polycrystalline film will open pores in the range of only 2 to 5 nm in our case using a FIB probe of 5 nm FWHM, but this ultimate resolution is not easy to reproducibly control, since the final pattern resolution is determined by the membrane grain size and orientation rather than the FIB probe size.

We also pointed out an optimum aspect ratio for the nanopores ranging between 6 to 7 for both SiN and SiC membranes having thicknesses in the range 10 to 100 nm.

From these preliminary experiments we learned that:

- Ultimate resolution of nanopores in thin amorphous membranes is ultimately determined by the membrane structure and thickness. Smaller or larger

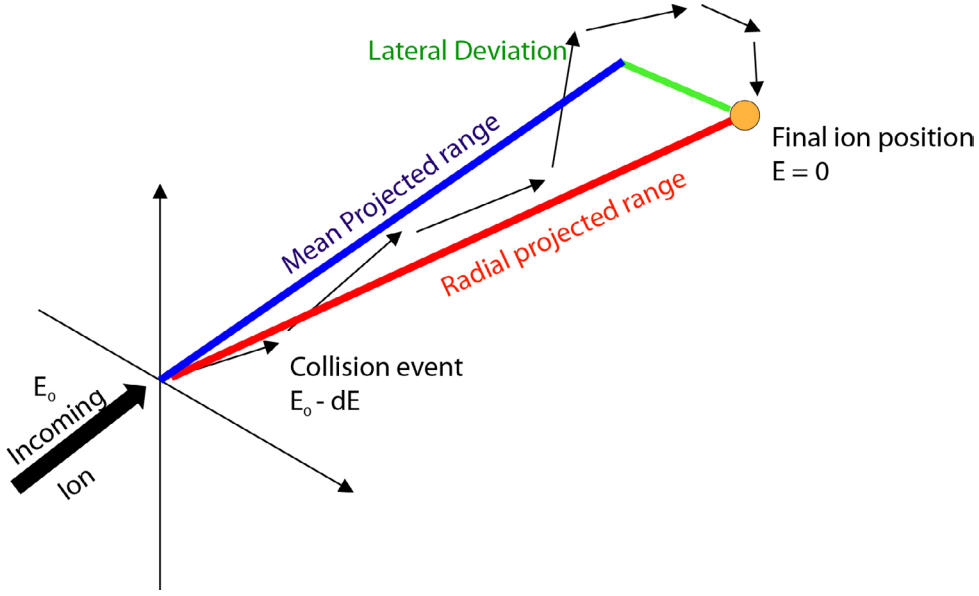

Figure 8: Schematic illustration of the development of a collision cascade. Obviously if the sample total thickness is below the particle mean projected range the incoming particle will be transmitted.

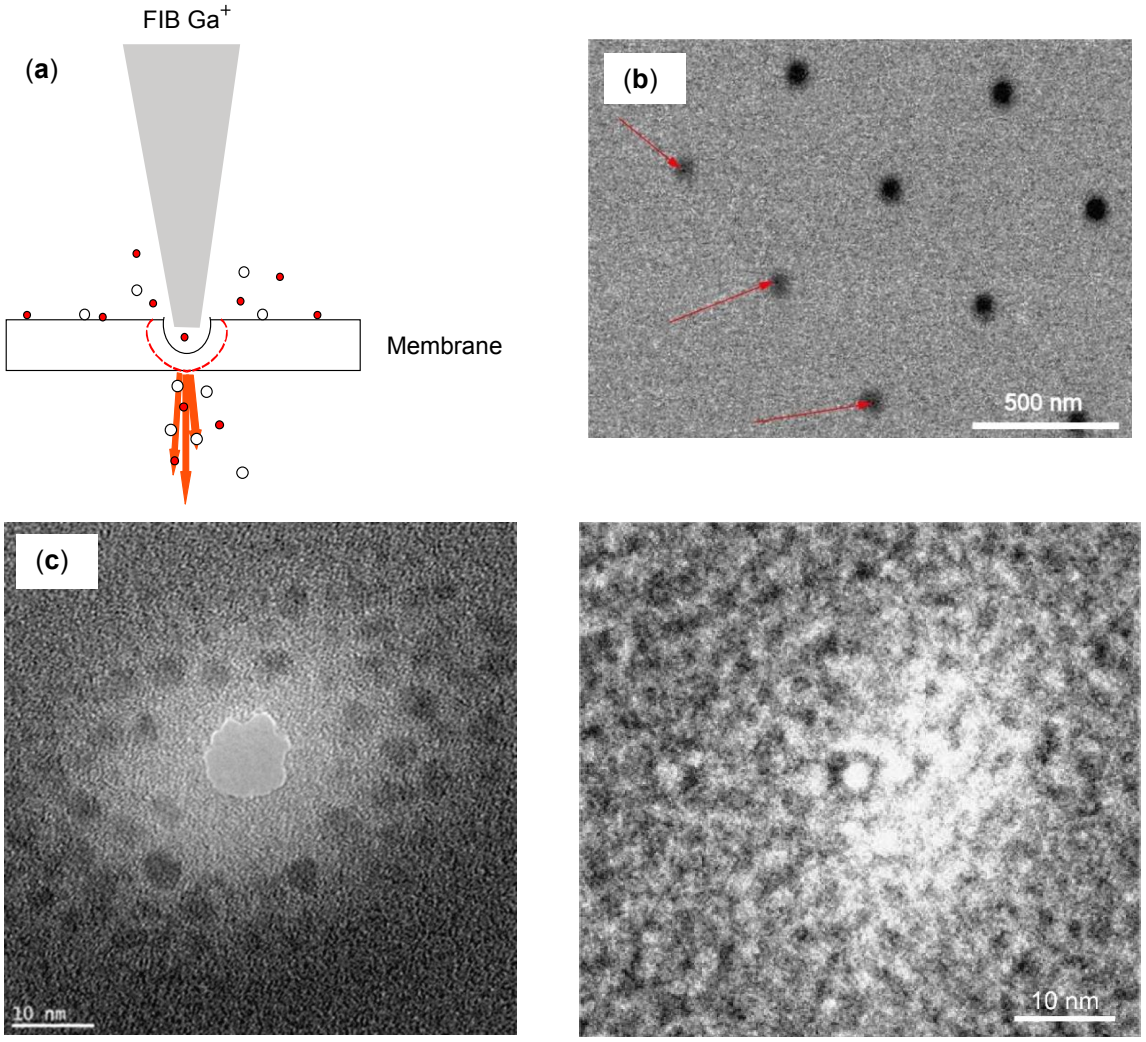

Figure 9: (a) Principle of the FIB processing method used for the ultra-thin membrane processing. (b) Array of nanopores drilled with increasing FIB doses used to calibrate the critical dwell time defining open nanopores. Low energy SEM imaging reveals sub-5nm openings (red arrows) in agreement with the SiO2 membrane grain size and roughness. (c) TEM images of a 8 nm open pore drilled in a 50 nm SiN membrane (left) and a of a 3 nm open pore drilled in a 20 nm thick SiC membrane (right) using a 5nm FWHM Ga+ 35 keV. Note the difference in grain structure between the two membrane materials.

grain sizes result in variable pore sizes and the same is true for local crystalline orientation of the grains.

– For exploring ultimate nanopore milling capabilities of our Ga-FIB technology, thinner membrane media (atomic level) and perfectly reproducible crystal orientations have to be preferred.

4.4.b. FIB patterning of suspended graphene nanostructures. Graphene is a strictly two-dimensional hexagonal lattice of carbon atoms with a thickness of one or a few atomic layers [47]. The motivation for our study arose from the observation that isolated atomically thin conducting membranes of graphene can be used for carving reproducible structures and overcoming the limitations of amorphous media detailed above.

The perspective of fabricating nanopores [48] or conductive nano-ribbons [49] with remarkable properties also attracted our interest. Indeed graphene and the related materials generate a considerable interest in materials science and condensed-matter physics. One crucial technological problem, that will govern future applicability of these “new” materials, is related to the patterning methods that need to be developed for preserving their exceptionally high crystallinity and electronic properties. We have evaluated the possibility to fabricate structures (holes, slits, ribbons) in graphene and hexagonal boron nitride (h-BN) atomically thin suspended sheets [50].

We have noticed important differences when comparing h-BN with graphene flakes for the resistance to

ion irradiation and found that the h-BN flakes were found to peel off even at moderate FIB imaging doses. Thus the focus and probe shaping sequences must be kept very short. Surprisingly the dwell time for milling nanopores does not differ significantly between graphene and h-BN flakes. For h-BN and graphene flakes of a few layers thicknesses, a 8nm hole engraved in the h-BN foil requires $6.75.10^4$ ions to be injected, and for a graphene (HOPG) a 7.8 nm hole is obtained with a point dose of 5.10^4 Ga^+ ions (30keV).

During our experimentations and observations, we have also checked for the presence of gallium ions in the vicinity of the drilled pores. Bright Field High Resolution STEM image of the region around FIB patterned pores were made for both for graphene and h-BN materials and subsequent Fourier Transform diffractograms clearly revealed that both the graphene and h-BN crystal structure were preserved in our attempts at sculpting graphene and h-BN suspended flakes when using our gallium FIB instrument and processing methodologies.

Regarding the ultimate lateral damages induced by the ion bombardment HR-TEM observations have revealed on the edges of nano-ribbons an amorphous region having a width of only 2.5 nm, perfectly aligned on the graphene crystal lattice. (i) Rolling effects were detected at the edges of the fabricated structures either in SEM and high resolution TEM. This effect is in agreement with theoretical predictions and recent observations of induced defects. But unfortunately this rolling effect made it almost impossible for us to probe the graphene integrity at the sculpted edges using a TEM.

(ii) We have also noted that cutting speeds for isolated lines in our exfoliated graphene films were dependent of the scanning directions. When sculpting a line in an exfoliated graphene flake suspended between two metal pads: If the scanning direction was parallel to the flake attachments the dose was found to be considerably lower (x2 up to x5) in comparison to a perpendicular direction on the same flake. Rather than attributing this reproducible behaviour to lattice orientations, we attributed these effects to residual stretching forces in the flake resulting from the exfoliation/deposition process. These tensile forces seem to favour a de-zipping effect of the flake into a ribbon.

- From this step we learned that it is possible to apply a FIB probe as a cleaving knife to split graphene nano-ribbons out of flakes along definite structural planes direction. This method based on the exploitation of the tensile strengths is a new way of using a pencil of ions to initiate a cleaving process.
- An important and unexpected finding of this study is that, in contrast to gallium-FIB engraving of dielectric or metallized silicon-based membranes, nanopores patterned in atomically thin sheets of graphene or h-BN have sizes that appear to be limited to around 8 nm. These materials exhibit unusual properties:
- High transparency. Atomically-thin flakes allow an important fraction of the incident gallium beam to be transmitted, generating a high secondary electron signal when impacting the sample holder metal surface.
- h-BN flakes are easily destroyed during imaging when the beam is digitally scanned over µm-sized area with only a few ions per point, but drilling a single nanopore in the same material require 10 millions of ions directed to a single pixel to produce a stable nanopore. This can be the result of the insulating properties of h-BN.
- We have verified that for atomically thin flakes of both graphene and h-BN the fabricated pores do not exhibit circular shapes for diameters below 10-15nm.

These observations suggest that reconstruction effects may occur and that a gallium ion dose threshold has to be deposited in order to pattern stable nanopores. Below a critical deposited dose, we were unable to observe any open circular nanopores in both graphene and h-BN atomically thin sheets. This effect has been already predicted using molecular dynamics simulations [51] and is currently under investigation in our team. In the light of our investigations nanopores were carved in such h-BN flakes using a dedicated gallium FIB nanowriter and this material appears very promising for biosensing applications.

4.5 Single ion implantation perspectives

In coll. with A. Balocchi, T. Amand, X. Marie et al. Université de Toulouse, INSA-CNRS-UPS, LPCNO, 135 avenue de Rangueil, 31077, Toulouse, France

We have recently demonstrated using a record-low number of gallium ions to create selectively spin filtering regions in non-magnetic InGaAs layers. Spin dependent recombination regions were selectively created in N-free InGaAs epilayers by our FIB technology inducing local implantation of gallium ions. The fabrication of spin dependent recombination (SDR) active regions in dilute nitrides compounds is usually achieved by epitaxial growth. SDR active quantum wells or epilayers can thus be produced with in-plane uniformity but without easy engineering possibilities of specific active region patterns. In this application the fabrication of the spin filtering

zones was achieved by FIB implantation to define 200 µm x 200 µm square patterns in the 50 nm thick InGaAs layer (Figure 10).

Reproducible and controlled effects were observed with Ga^+ irradiation ion doses ranging from 1.8×10^{12} cm^{-2} down to 1.8×10^{8} cm^{-2} giving respectively a few tens of ions per impact down to less than one ion in tens successive impacts [52]. This ultra-sensitive phenomenon resulting from the implantation of only a few ions opens the door to single ion implantation perspectives.

5 Conclusions and perspectives

The examples presented here suggest a major paradigm shift for FIB processing. Before these achievements, nano-fabrication with scanned focused ion beams, as a sequential process, was not expected to provide a mass-production capability of devices in terms of throughput and device or material integrity preservation. The success of our FIB approach in this application is due to the very high performance of our instrument, its capability to work "in-line" with standard lithography techniques, and to the high added value of our processing methodologies. One important effort we have tried to summarize in this article has been directed on understanding the limit of the Ga-FIB technology. This effort has allowed us develop, adapt and tune a technological response driven by scientific application requests in the form of a specific irradiation methodologies.

The combined performance of this instrument and of our processing methodologies have been evaluated against some of the most emblematic challenges in nanosciences moving from the classical "top-down" approach to "Bottom-up" and "guided organization". In the light of the results we have presented here, some better understanding has been gained on the limits of ion irradiation process at the nanoscale. Following this, FIB techniques with specific ion nature and energies now open the perspectives of nm-scaled lateral resolution and single-ion implantation. It is our opinion that FIB applications will now extend to new and promising challenges such as single-ion implantation for the development of Si-based MOSFET devices with quantum functionalities [53] or the creation of nitrogen vacancy (NV) centre a defect formed in diamond by one substitutional nitrogen atom and an adjacent vacancy. The NV centre is one of the most prominent candidates for room temperature quantum information processing [54].

As a perspective, it appears clearly to us that the reasons motivating the strong scepticism toward FIB technology have to be re-examined. It has to be agreed that the idea of using ions for nano-fabrication, which could have been considered as a pure dream only a few years ago, is now validated. The consequence is that FIB direct patterning techniques, previously deemed unable to enter the ambitious "nano" application field, has entered this domain and opened promising perspectives.

Thanks to a close feedback loop with experts in various scientific domains and highly sensitive analysis techniques we have then demonstrated, using such a FIB tool, that direct, efficient and clean materials nano-structuration could be reproducibly achieved and controlled when appropriate cares and sample configurations were selected.

In terms of perspectives, it is clear that the FIB technology remains promising and quite unexplored with respect to alternative ion natures, low ion landing energies and molecular ions engineering. In the light of the interest raised by the recent developments aiming at generating noble gas ions and or light ions, it is important to keep in mind that relatively heavy ions like gallium do keep the important advantage of benefitting of a shorter penetration depth and therefore reduced interaction volume in a given target. This advantage refers to localization of modifications at surface or in the vicinity of a surface, a characteristic that is of primary importance in nanosciences.

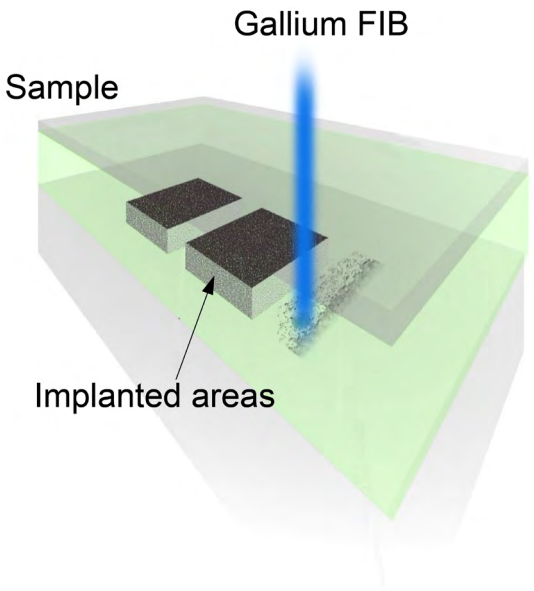

Figure 10: Schematic of the fabrication of the spin filtering zones by Focused Ion Beam implantation of Ga ions (35 ke, probe current 3 pA). Seven 200 µm side square regions were implanted in the 50 nm thick InGaAs layer with surface doses ranging from $1.8x10^{8}$ ions/cm² to $1.8x10^{12}$ ions/cm². Adapted from [52].

Acknowledgements: The author would like to express his thanks to all his colleagues that were involved in this research effort, with a special emphasis on his LPN-CNRS co-workers for their strong and continuous support over the years, to A. Septier and F. Miserey for their encouragements and guidance.

Special thanks to all the following collaborators:

- J. Ferré, J. Jamet A. Mougin of the Laboratoire de Physique des Solides, UMR CNRS 8502, Université Paris-Sud, F-91405 Orsay, France.
- B. Prevel, L. Bardotti, A. Perez, P. Mélinon, J.M. Benoit of the Institut Lumière Matière, UMR5306 CNRS, Université Claude Bernard Lyon 1, Domaine Scientifique de La Doua, Bâtiment Kastler, 10 rue Ada Byron, 69622 Villeurbanne, France,
- L. Auvray, F. Montel et al.Laboratoire Matière et Systèmes Complexes, CNRS - Université Paris Diderot, France
- A. Balocchi, T. Amand, X. Marie et al. Université de Toulouse, INSA-CNRS-UPS, LPCNO, 135 avenue de Rangueil, 31077, Toulouse, France.
- L. Bruchhaus and R. Jede, Raith GmbH, Konrad-Adenauer-Allee 8, 44263 Dortmund, Germany

This work was partially supported by the "Nano-fabrication with Focused Ion Beams" (Nano-FIB / G5RD-CT2000-00344), ANR "BioGraph'N" and "MIKADO" research projects.

References

[1] Yamamoto M., Sato M., Kyogoku H., Aita K., Nakagawa Y., Yasaka A., et al., Submicron Mask Repair Using Focused Ion Beam Technology, Proc. SPIE 0632, Electron-Beam, X-Ray, and Ion-Beam Technology for Submicrometer Lithographies V, 97 (June 30, 1986); doi:10.1117/12.963674

[2] Reyntjens S., Puers R., A review of focused ion beam applications in microsystem technology, J. Micromech. Microeng., 2001, 11, 287–300.

[3] Ziegler J., SRIM - the stopping and range of ions in matter, http://www.srim.org/.

[4] Levi-Setti R., Crow G., Wang Y.L., Parker N.W., Mittleman R., High-Resolution Scanning-Ion-Microprobe Study of Graphite and its Intercalation Compounds, Phys. Rev. Lett., 1985, 54, 2615.

[5] Orloff J., Focused Ion Beams, Sci. Am. Intl. Ed., 1991, 265, 74-79.

[6] Seliger R.L., Kubena R.L., Olney R.D., Ward J.W., Wang V., High-resolution, ion-beam processes for microstructure fabrication, J. Vac. Sci. Technol., 1979, 16, 1610.

[7] Beale M.I.J., Broughton C., Deshmukh V.G.I., Focused ion beams for lithography and direct doping in VLSI device fabrication, Microelectron. Eng., 1986, 4, 233-249.

[8] Lehrer et coll., EIPBN 2001, Washington, 2001.

[9] Gamo K., Miyake Y., Yuba Y., Namba S., Kasahara H., Sawaragi H., Aihara R, Defect study in GaAs bombarded by low-energy focused ion beams, J. Vac. Sci. Technol. B, 1988, 6, 2124.

[10] Hirayama Y., Susuki Y., Okamoto H., Compositional disordering and very-fine lateral definition of GaAs-AlGaAs superlattices by focused Ga ion beams, Surf. Sci., 1986, 174, 98-104.

[11] Yamamoto T., Yanagisawa J., Gamo K., Takaoka S., Murase K., Estimation of damage induced by focused Ga ion beam irradiation, Jpn. J. Appl. Phys., 1993, 32, 6268-6273.

[12 Kazazis D., Genner U., Gierak J. et al, to be presented at EIPBN conference 2014

[13] Gierak J., Focused ion beam technology and ultimate applications, Semicond. Sci. Technol., 2009, 24, 043001.

[14] Orloff J., Swanson L.W., Utlaut M., Fundamental limits to imaging resolution for focused ion beams, J. Vac. Sci. Technol. B, 1996, 14, 3759-3763.

[15] Kubena R.L., Ward J.W., Stratton F.P., Joyce R.J., Atkinson G.M., A low magnification focused ion beam system with 8 nm spot size, J. Vac. Sci. Technol. B, 1991, 9, 3079.

[16] Vieu C., Ben Assayag G., Gierak J., Observation and simulation of focused ion beam induced damage, Nucl. Instr. Meth. Phys. Res., 1994, 93, 439-446.

[17] Orloff J., Comparison of optical design approaches for use with liquid metal ion sources, J. Vac. Sci. Technol. B, 1987, 5, 175.

[18] Kruit P., Jiang X.R., Influence of Coulomb interactions on choice of magnification, aperture size, and source brightness in a two lens focused ion beam column, J. Vac. Sci. Technol. B, 1996, 14, 1635.

[19] Smith N.S., Tesch P.P., Martin N.P., Boswel R.W., New Ion Probe for Next Generation FIB, SIMS, and Nano-Ion Implantation, Microscopy Today, 2009, 17, 18-22.

[20] Carleson, Routh, Kelley, Young, High-Throughput, Site-Specific Inspection of 3D Interconnects using Plasma FIB Technology, 3D-IC Metrology Workshop, San Francisco CA USA, July 11, 2012.

[21] Levi-Setti R., Proton scanning microscopy: Feasibility and promise, in Scanning Electron Microscopy/1974, Johari O., Corvin I., ed., IIT Research Institute, Chicago, Ill., 1974, 125-134.

[22] Müller E.W., Das Feldionenmikroskop, Zeitschrift für Physik, 1951, 131, 136-142.

[23] Suvorov V.G., Forbes R.G., Theory of minimum emission current for a non-turbulent liquid-metal ion source, Microelectron. Eng., 2004, 73-74, 126-131.

[24] Van Es J.J., Gierak J., Forbes R.G., Suvorov V.G., Van den Berghe T., Dubuisson P., et al., An improved gallium liquid metal ion source geometry for nanotechnology, Microelectron. Eng., 2004, 73-74, 132-138.

[25] Sudraud P., Ben Assayag G., Bon M., Focused-ion-beam milling, scanning-electron microscopy, and focused-droplet deposition in a single microcircuit surgery tool, J. Vac. Sci. Technol. B, 1988, 6, 234.

[26] Gnauck P., Vacuum's Best 2005: Special Issue of "Vacuum in Research and Practice", 2005.

[27] Thoms S., Electron Beam Lithography, in Nanofabrication Handbook, Cabrini S., Kawata S., ed., CRC Press, 2012.

[28] Gierak J., Jede R., Hawkes P., Nanolithography with Focused Ion Beams, in Nanofabrication Handbook, Cabrini S., Kawata S., ed., CRC Press, 2012.

[29] NanoFIB 2004, EC research project See: ftp://ftp.cordis.europa.eu/pub/nanotechnology/docs/n_s_nanofib_27052002.pdf

[30] Gierak J., Septier A., Vieu C., Design and realization of a very high-resolution FIB nanofabrication instrument, Nucl. Instr. and Meth. A, 1999, 427, 91-98.
[31] Lencova B., http://www.lencova.com/; Munro E., http://www.mebs.co.uk/.
[32] Sugimoto Y., Akita K., Taneya M., Wawanishi H., Aihara R., Watahiki T., A multichamber system for in situ lithography and epitaxial growth of GaAs, Rev. Sci. Instrum., 1991, 62, 1828-1835.
[33] Chen C.H., Green D.L., Hu E.L., Ibbestson J.P., Petroff P.M., Radiation enhanced diffusion of low energy ion-induced damage, Appl. Phys. Lett., 1996, 69, 58-60.
[34] Ben Assayag G., Vieu C., Gierak J., Sudraud P., Corbin A., New characterization method of ion current-density profile based on damage distribution of Ga+ focused-ion beam implantation in GaAs, J. Vac. Sci. Technol. B, 1993, 11, 2420-2426.
[35] Gierak J., Ben Assayag G., Schneider M., Vieu C., Marzin J.Y., 3D defect distribution induced by focused ion beam irradiation at variable temperatures in a GaAsGaAlAs multi quantum well structure, Microelectron. Eng., 1996, 30, 253-256.
[36] Chappert C., Bernas H., Ferre J., Kottler V., Jamet J.P., Chen Y., et al., Planar Patterned Magnetic Media Obtained by Ion Irradiation, Science, 1998, 280, 1919-1922.
[37] Johnson W.L., Cheng Y.T., Van Rossum M., Nicolet M., When is thermodynamics relevant to ion-induced atomic rearrangements in metals?, Nucl. Instrum. Methods Phys. Res. B, 1985, 7, 657-665.
[38] Albrecht M., Rettner C.T., Moser A., Best M.E., Terris B.D., Recording performance of high-density patterned perpendicular magnetic media, Appl. Phys. Lett., 2002, 81, 2875-2877.
[39] Ruotolo A., Wiebel S., Jamet J.P., Vernier N., Pullin D., Gierak J., Ferré J., Magneto-optical microscopy as a favourite tool to probe focused ion beam patterning at low dose, Nanotechnology, 2006, 17, 3308–3312.
[40] Rau N., Stratton F., Fields C., Ogawa T., Neureuther A., Kubena R., Willson G., Shot-noise and edge roughness effects in resists patterned at 10 nm exposure, J. Vac. Sci. Technol. B, 1998, 16, 3784.
[41] Mélinon P., Hannour A., Bardotti L., Prével B., Gierak J., Bourhis E., et al., Ion beam nanopatterning in graphite: characterization of single extended defects, Nanotechnology, 2008, 19, 235305.
[42] Perez A., Bardotti L., Prevel B., Jensen P., Treilleux M., Mélinon P., et al., Quantum-dot systems prepared by 2D organization of nanoclusters preformed in the gas phase on functionalized substrates, New J. Phys., 2002, 4, 76.
[43] Prével B., Benoit J.M., Bardotti L., Mélinon P., Ouerghi A., Lucot D., et al., Nanostructuring graphene on SiC by focused ion beam: effect of the ion fluence, Appl. Phys. Lett., 2011, 99, 083116.
[44] Carleson, Routh, Kelley, Young, 3D-IC Metrology Workshop, San Francisco CA USA July 11, 2012 www.sematech.org/meetings/archives/
[45] Biance A.L., Gierak J., Bourhis E., Madouri A., Lafosse X., Patriarche G., et al., Focused ion beam sculpted membranes for nanoscience tooling, Microelectron. Eng., 2006, 83, 1474-1477.
[46] Gierak J., Madouri A., Biance A.L., Bourhis E., Patriarche G., Ulysse C., et al., Sub-5 nm FIB direct patterning of nanodevices, Microelectron. Eng., 2007, 84, 779-783.
[47] Geim A.K., Graphene: status and prospects, Science, 2009, 324, 1530–1534.
[48] Garaj S., Hubbard W., Reina A., Kong J., Branton D., Golovchenko J.A., Graphene as a subnanometre trans-electrode membrane, Nature, 2010, 467, 190-193.
[49] Lucot D., Gierak J., Ouerghi A., Bourhis E., Faini G., Mailly D., Deposition and FIB direct patterning of nanowires and nanorings into suspended sheets of graphene, Microelectron. Eng., 2009, 86, 882-884.
[50] Hemamouche A., Morin A., Bourhis E., Toury B., Tarnaud E., Mathé J., et al., FIB patterning of dielectric, metallized and graphene membranes: A comparative study, Microelectron. Eng., 2014, 121, 87-91.
[51] Li W., Liang L., Zhao S., Zhang S., Xue J., Fabrication of nanopores in a graphene sheet with heavy ions: A molecular dynamics study, J. Appl. Phys., 2013, 114, 234304; Kotakoski J., Lehtinen O.J., Nanomachining Graphene with Ion Irradiation, MRS Proceedings 1259E, 2010, 1259-S18-02.
[52] Nguyen C.T., Balocchi A., Lagarde D., Zhang T.T., Carrère H., Mazzucato S., et al., Fabrication of an InGaAs spin filter by implantation of paramagnetic centers, Appl. Phys. Lett., 2013, 103, 052403.
[53] McCallum J.C., Jamieson D.N., Yang C., Alves A.D., Johnson B.C., Hopf T., et al., Single-Ion Implantation for the Development of Si-Based MOSFET Devices with Quantum Functionalities, Adv. Mater. Sci. Eng., 2012, 2012, 272694. doi:10.1155/2012/272694
[54] Aharonovich I., Greentree A.D., Prawer S., Diamond photonics, Nature Photon., 2011, 5, 397-405.